FULL PAPER

Dalton
www.rsc.org/dalton

External heavy-atom effect of gold in a supramolecular acid–base π stack

Ahmed A. Mohamed,[a] **Manal A. Rawashdeh-Omary,**[b] **Mohammad A. Omary***[b] **and John P. Fackler, Jr.***[a]

[a] *Department of Chemistry, Texas A & M University, College Station, Texas, 77843, USA. E-mail: fackler@mail.chem.tamu.edu*
[b] *Department of Chemistry, University of North Texas, Denton, TX, 76203, USA. E-mail: omary@unt.edu*

Received 5th May 2005, Accepted 20th June 2005
First published as an Advance Article on the web 4th July 2005

DOI: 10.1039/b506319a

The nucleophilic trinuclear Au(I) ring complex $Au_3(p\text{-tolN=COEt})_3$, **1**, forms a sandwich adduct with the organic Lewis acid octafluoronaphthalene, $C_{10}F_8$. The $\mathbf{1}\cdot C_{10}F_8$ adduct has a supramolecular structure consisting of columnar interleaved 1 : 1 stacks in which the $Au_3(p\text{-tolN=COEt})_3$ π-base molecules alternate with the octafluoronaphthalene π-acid molecules with distances between the centroid of octafluoronaphthalene to the centroid of **1** of 3.458 and 3.509 Å. The stacking with octafluoronaphthalene completely quenches the blue photoluminescence of $Au_3(p\text{-tolN=COEt})_3$, which is related to inter-ring Au–Au bonding, and leads to the appearance of a bright yellow emission band observed at room temperature. The structured profile, the energy, and the lifetime indicate that the yellow emission of the $\mathbf{1}\cdot C_{10}F_8$ adduct is due to monomer phosphorescence of the octafluoronaphthalene. The 3.5 ms lifetime of the yellow emission of $\mathbf{1}\cdot C_{10}F_8$ is two orders of magnitude shorter than the lifetime of the octafluoronaphthalene phosphorescence, thus indicating a strong gold heavy-atom effect. The diffuse-reflectance spectrum of the solid adduct shows new absorptions that are red-shifted from the absorptions of the monomeric organic and inorganic components alone, indicating charge transfer. Luminescence excitation spectra suggest that these new absorptions represent the major excitation route that leads to the yellow luminescence of $\mathbf{1}\cdot C_{10}F_8$, which is different from the conventional heavy-atom effect in which the phosphorescence route entails simply the enhancement of the S_1–T_1 intersystem crossing of the organic compound.

Introduction

Extended linear chain compounds that contain metal atoms exhibit important aspects in chemical bonding as well as fascinating chemical and physical properties.[1–3] Many classes of coordination compounds that exhibit such structures have been reported, which has given rise to advances in several fundamental and applied research aspects in areas that include supramolecular architecture, acid–base chemistry, metallophilic bonding, luminescent materials, optical sensing, and various optoelectronic applications. Among the many recent developments in this area are reports about a vapochromic light-emitting diode from linear chain Pt(II)/Pd(II) complexes,[4] a luminescent switch consisting of an Au(I) dithiocarbamate complex that possesses a luminescent linear chain form only in the presence of vapors of organic solvents,[5] a vapochromic complex, $\{Tl[Au(C_6Cl_5)_2]\}_n$, that shows a quantum dot effect and reversible color changes upon binding to volatile organics,[6] a modified form of Magnus' green salt, $[(NH_3)_4Pt][PtCl_4]$, that exhibits semiconducting properties,[7] a variety of d^8 complexes that interact with inorganic[8] and organic[9] molecules to form donor–acceptor extended-chain adducts with interesting conducting and/or magnetic properties, and new interesting complexes that exhibit strong heterobimetallic bonding between different closed-shell metal ions.[10,11] A specially intriguing class of linear-chain species involves trinuclear d^{10} complexes, which have garnered considerable interest in recent years owing in large part to their fascinating luminescence properties. For example, Balch and co-workers reported that a trinuclear carbeniate Au(I) complex exhibits "solvoluminescence", *i.e.* it produces spontaneous orange emission upon contact with solvent in samples that had been irradiated with long-wavelength UV light.[12a] The same and related complexes have been found to form charge-transfer complexes with nitro-9-fluorenones[12b] and some form hourglass figures on standing or when placed in an acid.[12c] Gabbaï and co-workers have reported that a trinuclear Hg(II) complex forms 1 : 1 adducts with aromatic hydrocarbons, which become brightly phosphorescent at room temperature due to a mercury heavy-atom effect.[13,14] Recently, Omary and Dias have shown that trinuclear Cu(I) pyrazolato complexes exhibit bright emissions that can be tuned to multiple luminescence colors across the visible region by varying the temperature, solvent, or concentration.[15]

We have been studying trinuclear Au(I) compounds with aromatic-substituted imidazolate and carbeniate bridging ligands. These compounds are colorless and do not form extended-chain structures. However, it has been shown that they can form sandwich adducts with a variety of electrophiles to produce supramolecular chains (Chart 1) that exhibit interesting bonding and optoelectronic properties that are related to the chain structure.[16–21] While most adducts show 2 : 1 assemblies, we recently communicated a notable exception for the $\mathbf{1}\cdot C_6F_6$ adduct, which assembled in a 1 : 1 ratio and is non-luminescent. Here, we report a detailed structural and photophysical study about the formation of a sandwich adduct of **1** with octafluoronaphthalene ($C_{10}F_8$). The new $\mathbf{1}\cdot C_{10}F_8$ adduct forms a 1 : 1 supramolecular stack and exhibits phosphorescence characteristic of the organic molecule due to a gold heavy-atom effect. The photophysical data illustrate a different excitation route in $\mathbf{1}\cdot C_{10}F_8$ from the conventional heavy-atom effect in organic molecules and show signature bands for the secondary π interactions in the absorption and not the emission process of the adduct. A discussion of the puzzling differences in the luminescence and structural properties of the various 1 : 1 and 1 : 2 donor–acceptor stacks shown in Chart 1 is also presented.

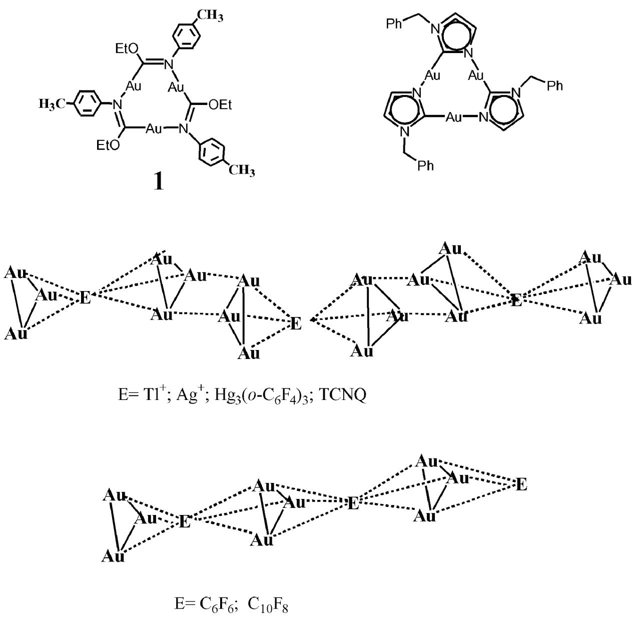

Chart 1 Structures of the trinuclear Au^I compounds studied and their adducts with various electrophiles.

Experimental

General

Octafluoronaphthalene (96%) was obtained from Matrix Scientific and used as received. Synthesis of **1** was performed according to a published procedure.[22] Dichloromethane was distilled over P_4O_{10}.

Synthesis

The adduct **1**·$C_{10}F_8$ was synthesized by dissolving 100 mg (0.09 mmol) of **1** in 2 mL of dichloromethane and adding to it 25 mg (0.09 mmol) of octafluoronaphthalene. The solution was stirred for 1 h and diethyl ether added to form a white product. In another preparation, an excess of octafluoronaphthalene was added to **1** dissolved in dichloromethane and the solvent evaporated. The excess octafluoronaphthalene sublimed at room temperature to leave a white product. Colorless single crystals used in the crystallographic and luminescence studies were grown by slow evaporation from dichloromethane. Yield (107 mg, 87%), mp 198–200 °C (mp of octafluoronaphthalene is 89–90 °C and of **1** is 180 °C). ^{19}F NMR: 20 (s) and 28 (s) ppm. Anal. Calc. (found) for $C_{40}H_{36}Au_3F_8N_3O_3$: C, 35.57 (35.14); H, 2.68 (2.41); N, 3.11 (3.08); F, 11.26 (11.97)%.

Physical measurements

The luminescence and diffuse-reflectance measurements were carried out at the University of North Texas for crystalline material carefully examined by optical microscopy. Steady-state luminescence spectra were acquired with a PTI QuantaMaster Model QM-4 scanning spectrofluorometer equipped with a 75-watt xenon lamp, emission and excitation monochromators, excitation correction unit, and a PMT detector. The emission and excitation spectra were corrected for the wavelength-dependent detector response and lamp output, respectively. Lifetime data were acquired using a nitrogen laser interfaced with a tunable dye laser and a frequency doubler, as part of fluorescence and phosphorescence sub-system add-ons to the PTI instrument. The 337.1 nm line of the N_2 laser was used directly to generate the time-resolved data. Luminescence measurements at 77 K were acquired by placing the crystalline samples in a Suprasil quartz capillary tube inserted into a liquid-nitrogen Dewar flask with a Suprasil quartz cold finger, which was positioned and aligned in the sample compartment of the fluorometer. Electronic absorption and diffuse-reflectance spectra were acquired using a Perkin-Elmer Lambda 900 double-beam UV/VIS/NIR spectrophotometer. Absorption measurements were carried out for freshly-prepared solutions in HPLC-grade CH_3CN using matching 1-cm or 1-mm Suprasil quartz cuvettes obtained from Wilmad for the sample and the blank simultaneously in the double-beam setup. The solid-state diffuse-reflectance spectra were measured using a 150-mm integrating sphere (by Labsphere) accessory to the Lambda 900 spectrophotometer. This was done by packing crystals of the compound in a 0.1 mm Suprasil quartz cuvette (Wilmad).

Melting points were measured on a Unimelt capillary melting point apparatus and are reported uncorrected. ^{19}F NMR spectra were obtained on a Varian XL-200 spectrometer, or a Varian UnityPlus-300 spectrometer. ^{19}F NMR data are expressed in parts per million (ppm) and referenced externally to $CFCl_3$.

Structure determination

Data were collected using a Siemens (Bruker) SMART CCD (charge coupled device) based diffractometer equipped with a LT-2 low-temperature apparatus operating at 110 K. A suitable crystal was chosen and mounted on a glass fiber using cryogenic grease. Data were measured using omega scans of 0.3° per frame for 60 s, such that a hemisphere was collected. The first 50 frames were recollected at the end of data collection as a monitor for decay. No decay was detected. Cell parameters were retrieved using SMART software and refined using SAINT on all observed reflections.[23] Data reductions were performed using SAINT software.[24] Absorption corrections were applied using SADABS.[25] The structure was solved by direct methods using SHELXS-97 and refined by least squares on F^2, with SHELXL-97 incorporated in SHELXTL-PC V 5.03.[26,27] The structure was determined in the noncentric space group $P2_12_12_1$ (Flack parameter = 0.000(14)) by analysis of systematic absences. Hydrogen atom positions were calculated by geometrical methods and refined as a riding model.

Crystal data. $C_{40}H_{36}Au_3F_8N_3O_3$, M_r = 1349.62, unit-cell dimensions: a = 7.292(2), b = 21.289(6), c = 25.589(7), V = 3972.7(19) Å^3, Z = 4, T = 110 K, μ = 11.131, number of reflections measured: 6601, R_{int} = 0.0531, $R1$ = 0.0386, $wR2$ = 0.0968 (all data). The 342 restraints were developed by using ISOR values of 0.005 on C8 and C18 with 49 omitted reflections.

CCDC reference number 270181.

See http://dx.doi.org/10.1039/b506319a for crystallographic data in CIF or other electronic format.

Results and discussion

Synthesis of the 1·$C_{10}F_8$ adduct

The reaction of **1** with octafluoronaphthalene in dichloromethane forms the sandwich complex described here. The white product shows a strong yellow luminescence at room temperature under UV light. The ^{19}F NMR spectra for nearly saturated solutions of **1**·$C_{10}F_8$ in $CDCl_3$ show two singlet peaks at the same chemical shift (20 and 28 ppm) as those observed for $C_{10}F_8$ alone in $CDCl_3$ indicative of dissociation in solution. The $C_{10}F_8$ moiety melts at ~90 °C and the title complex melts at ~200 °C. Heating the **1**·$C_{10}F_8$ adduct at 65 °C results in a loss of the yellow luminescence within 3 min and, instead, a blue luminescent material is produced characteristic of the trinuclear starting material, **1**.[20] Cooling the solid sample to room temperature followed by adding drops of $C_{10}F_8$ in dichloromethane regenerates the yellow luminescence. The process was repeated three times without loss of the yellow luminescence.

Table 1 Selected bond distances (Å) and angles (°) for $\mathbf{1}\cdot C_{10}F_8$

Au(2)–C(8)	1.925(11)	Au(2)–N(2)	2.055(9)
Au(2)–C(18)	1.975(11)	Au(2)–Au(3)	3.2790(9)
Au(2)–Au(1)	3.2796(10)	Au(3)–C(18)	1.975(11)
Au(3)–N(3)	2.058(9)	Au(3)–Au(1)	3.3368(9)
Au(1)–C(28)	1.960(12)	Au(1)–N(1)	2.055(10)
C(39)–C(40)	1.421(17)		
C(8)–Au(2)–N(2)	177.7(4)	Au(3)–Au(2)–Au(1)	61.164(12)
C(18)–Au(3)–N(3)	178.4(4)	Au(2)–Au(3)–Au(1)	59.43(2)
C(28)–Au(1)–N(1)	178.7(4)	Au(2)–Au(1)–Au(3)	59.408(19)

Structural properties

The adduct $\mathbf{1}\cdot C_{10}F_8$ crystallizes in the noncentric orthorhombic space group $P2_12_12_1$. It is noted that $\mathbf{1}\cdot C_{10}F_8$ satisfies an important requirement for second-order NLO properties to appear with photoluminescent materials. Noncenteric space groups are relatively uncommon in inorganic compounds. Selected bond distances and angles are presented in Table 1. The molecular structure of $\mathbf{1}\cdot C_{10}F_8$ is shown in Fig. 1 and the stacking pattern is shown in Fig. 2. The Au · · · Au intramolecular interactions in **1** (3.224, 3.288, 3.299 Å) become longer upon adduct formation in $\mathbf{1}\cdot C_{10}F_8$ (3.279, 3.280, 3.337 Å). The longest Au · · · Au interaction of 3.337 Å is parallel to the plane passing through C(39)–C(40) in $C_{10}F_8$. A weak interaction between the fluorine and gold atoms of ~3.5 Å exists, which probably plays a role in the adduct stabilization. The change in Au–C and Au–N distances on going from **1** to $\mathbf{1}\cdot C_{10}F_8$ is negligible. There is essentially no change in the bond distances of aromatic C–C bonds in the naphthalene ring, consistent with Gabbai's observations for $[Hg_3(C_6F_4)_3]\cdot C_{10}H_{10}$.[13,14]

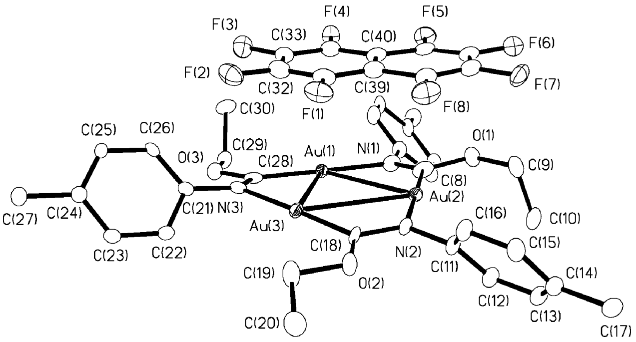

Fig. 1 ORTEP (50%) of $\mathbf{1}\cdot C_{10}F_8$.

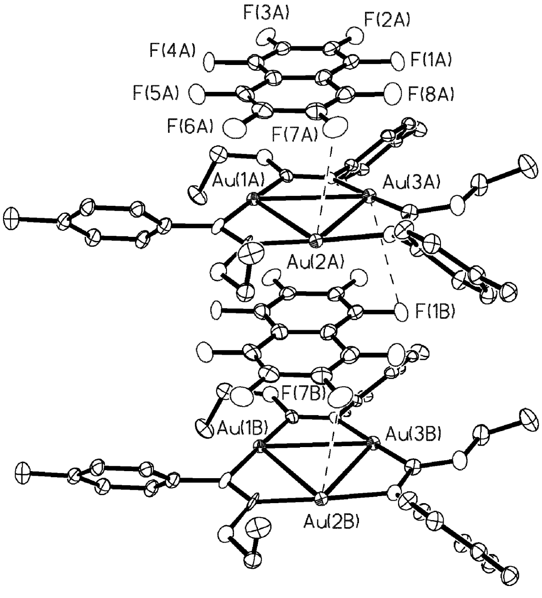

Fig. 2 Packing diagram of $\mathbf{1}\cdot C_{10}F_8$ showing the Au · · · F interaction.

The interactions between Au and F (3.458–3.509 Å) are probably augmented by electrostatic forces between the trinuclear entities and the $C_{10}F_8$ rings. The eight F atoms participate in intrastack $H_{tolyl}\cdots F$ contacts that range between 2.478 and 2.9993 Å. The F · · · H interactions appear to be an important factor in forming a short-range supramolecular structure. The octafluoronaphthalene molecules of one stack lie closer to the trinuclear molecules of adjacent stacks, but not exactly opposite to them. The various interactions induce Au–C–N–Au torsion angles of 6.55–11.71° in the trinuclear complex.

The distance between the centroid of $C_{10}F_8$ to the centroid of **1** is 3.509 Å compared to the slightly longer distance of 3.565 Å in $\mathbf{1}\cdot C_6F_6$. Perfluoroaromatic molecules are known to behave as electron acceptors and able to form compounds by interaction with electron rich trinuclear gold complexes. The fact that no significant change in the distances in the fluorinated naphthalene rings after intercalation is augmented by a recent report by Schafer and Cotton.[28] They showed that the neutral and anion $C_{10}F_8$ possess D_{2h} and the electron affinity of the neutral species is 1.01 eV compared to 0.69 eV for hexafluorobenzene. The larger electron affinity of $C_{10}F_8$ than that of C_6F_6 explains the shorter interplanar separation in $\mathbf{1}\cdot C_{10}F_8$ compared to $\mathbf{1}\cdot C_6F_6$.

The metallocycles are puckered and irregular in both the dimeric **1** and the $\mathbf{1}\cdot C_{10}F_8$ adduct. The three angles in the Au_3 unit are nearly equal, ~60°. The complex packs in the slipped stacks face-to-edge. The naphthalene rings are slipped such that one of the fused rings sits atop the trinuclear center and the other ring below another trinuclear center. The slip angle between the naphthalene rings is ~17°.

Photophysical properties

The structured blue emission of **1** is related to intermolecular Au–Au interactions in its dimeric crystallographic form.[19,20] Hence, the luminescence is quenched in 1 : 1 adducts of **1** with organic Lewis acids. In the case of the **1**·hexafluorobenzene adduct reported earlier, the adduct is not luminescent and exposure of the Au_3 solid compound to vapors of C_6F_6 quenches its luminescence within minutes.[20] In the case of the $\mathbf{1}\cdot C_{10}F_8$ adduct described here, a bright yellow structured emission band is observed even at ambient temperature and the vibronic structure becomes more resolved upon cooling to 77 K. Fig. 3 shows that the profile of the emission spectrum of crystals of $\mathbf{1}\cdot C_{10}F_8$ at 77 K is essentially the same as that of crystals of uncomplexed octafluoronaphthalene but with a slight red shift. At ambient temperature, the yellow organic-centered luminescence is very bright for $\mathbf{1}\cdot C_{10}F_8$ but undetectable for solid octafluoronaphthalene. Lifetime measurements show that the yellow luminescence of $\mathbf{1}\cdot C_{10}F_8$ is phosphorescence. Fig. 4 shows that the decay curve at 550 nm shows a single exponential fit with $\tau = 3.57 \pm 0.07$ ms. The magnitude of the lifetime does not change significantly with variations in either the laser excitation wavelength or the monitored emission wavelength. The luminescence intensity and lifetime both increase upon cooling. This is as expected because of the corresponding decrease in the rate constant of the non-radiative decay.

The structured profile, energy, and lifetime of the yellow emission of the $\mathbf{1}\cdot C_{10}F_8$ adduct indicate that the emission is monomer phosphorescence of the octafluoronaphthalene, for which the energy of the $T_1 \rightarrow S_0$ radiative transition is red-shifted only slightly. The 3.57 ms lifetime of the yellow emission of $\mathbf{1}\cdot C_{10}F_8$ is two orders of magnitude shorter than the lifetime of the octafluoronaphthalene phosphorescence, which was reported by different authors to be in the range of 0.25–0.38 *seconds* in frozen glasses.[29–31] The brightness of the yellow phosphorescence at room temperature for the $\mathbf{1}\cdot C_{10}F_8$ solid adduct along with the great reduction in the triplet lifetime compared to free octafluoronaphthalene are indicative of a strong gold heavy-atom effect. The slight red shift in the emission energy of $\mathbf{1}\cdot C_{10}F_8$ is also a known consequence of the heavy-atom

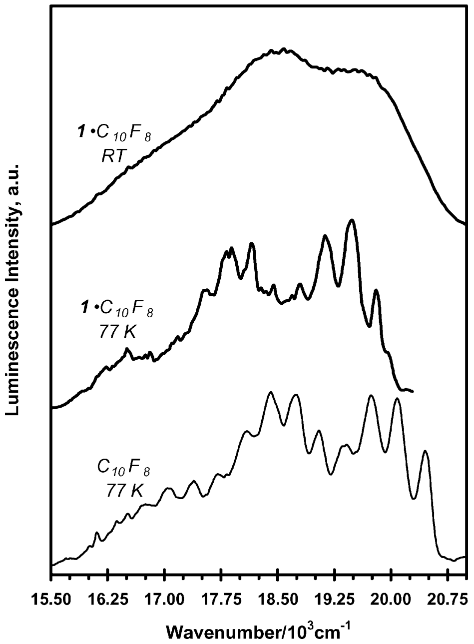

Fig. 3 Emission spectra of single crystals of the **1**·$C_{10}F_8$ stacked adduct and solid $C_{10}F_8$. No luminescence was detected at room temperature from solid $C_{10}F_8$.

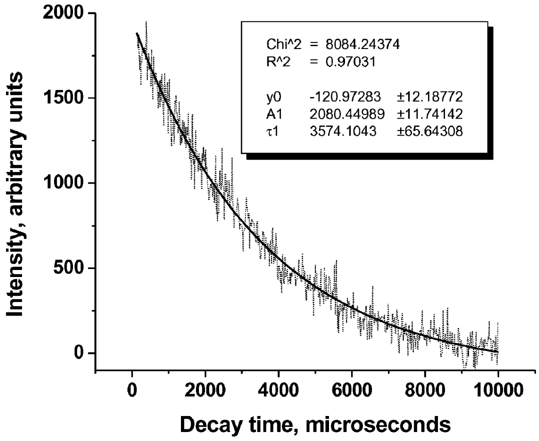

Fig. 4 Phosphorescence decay curve for the yellow emission band of single crystals of the **1**·$C_{10}F_8$. The emission is monitored at 550 nm generated with 337.1 nm pulsed N_2 laser excitation.

effect.[29,31] The interactions between **1** and naphthalene are secondary π interactions, as evidenced by the relatively long crystallographic distances between the planes of the two components (~3.5 Å between the centroids; *vide supra*). The energies of such interactions have been estimated to be in the range of only 1–2 kcal mol^{-1} in similar systems.[32,33] Hence, one can consider the heavy-atom effect seen here for the **1**·$C_{10}F_8$ adduct to be more comparable to the external heavy-atom effect known for organic compounds when a heavy atom is present in the luminophore environment (*e.g.*, in the solvent, host matrix, or "through space" interactions within the molecule), as opposed to the internal heavy-atom effect where a heavy atom is involved in a direct covalent bonding to the luminophore.[34–38] The external heavy-atom effect in organic compounds usually leads to a modest decrease in phosphorescence lifetimes while this decrease is much more significant in the case of the internal heavy-atom effect. For example, comparing (in a diethyl ether–isopentane–ethanol 5 : 5 : 2 glass) naphthalene ($\tau^P = 2.4$ s) with 1-bromonaphthalene and with norbornyl bromide fused to naphthalene (with the Br over the naphthalene) reduces the lifetime to 0.014 s and 0.77 s, respectively, due to internal and external heavy-atom effects.[34,35] The reduction in phosphorescence lifetime seen for **1**·$C_{10}F_8$ to ms levels due to an external heavy-atom effect of gold is much more significant than the common reduction in τ^P due to external heavy-atom effects and is more comparable to the reduction in τ^P due to internal heavy-atom effects. The spin–orbit coupling "ζ" parameter for the 5d orbital of Au(I) is 5100 cm^{-1},[39] comparable to the ζ values for the Br and I atoms of 2460 and 5700 cm^{-1}, respectively.[35,40] The internal heavy-atom effect in α-iodonaphthalene leads to $\tau^P = 2$ ms.[35] Meanwhile, lifetime data recently communicated by Omary and Gabbaï show τ^P values on the order of 10^{-1}–10^{0} ms for several 1 : 1 adducts of electron-rich aromatic hydrocarbons (naphthalene, biphenyl, pyrene) with the macrocyclic Lewis acid [μ-(*o*-C_6F_4)$_3$$Hg_3$].[14] Therefore, it is reasonable to conclude that secondary π interactions of aromatic luminophores with trinuclear complexes of 5d^{10} heavy metal ions lead to an unusually strong external heavy-atom effect that is comparable to the internal heavy-atom effect in organic compounds. The long-range ordering of the acid–base stacks, in which each organic triplet emitter is surrounded by six heavy metal atoms, is likely the major contributing factor to the unusually strong external heavy-atom effect seen here. This effect, however, is smaller than the internal effect in which metals are involved in coordinate covalent bonds with the organic moiety, wherein τ^P values of 10^1–10^2 μs are common for ligand-centered emissions in 5d^{10} complexes[41] and even in lighter 3d^{10} and 4d^{10} complexes.[42] The phosphorescence lifetimes are even shorter for metal-centered emissions, wherein τ^P values of a few μs and even 10^2 ns are quite common, *e.g.* for Au(I) complexes that show gold-centered emissions.[43]

In order to gain insight into the photophysical processes that lead to the enhanced phosphorescence in **1**·$C_{10}F_8$, absorption, diffuse-reflectance, and luminescence excitation spectra were obtained. Fig. 5 shows the diffuse-reflectance spectrum of the solid adduct **1**·$C_{10}F_8$. Because the adduct stacks in a 1 : 1 manner, the diffuse-reflectance data are compared with the absorption spectra for dilute solutions of **1** and of $C_{10}F_8$, which represent monomers of these species. Fig. 5 shows the **1**·$C_{10}F_8$ adduct exhibits not only absorptions characteristic of its two monomer components, but also new red-shifted features (designated by arrows) that extend the absorption edge of the adduct to approach the visible region. Luminescence excitation spectra suggest that these new absorptions represent the major excitation route that leads to the yellow luminescence of **1**·$C_{10}F_8$. Fig. 6 shows that distinct luminescence excitation peaks appeared near 335 and 360 nm for **1**·$C_{10}F_8$, which correspond to the red-shifted diffuse-reflectance features. The fact that these new features become much more clearly discernible in the luminescence excitation spectrum than they were in the diffuse reflectance spectrum indicates the central role played by their corresponding transitions in the excitation route of **1**·$C_{10}F_8$. For comparison, Fig. 6 also shows the luminescence excitation spectrum of $C_{10}F_8$

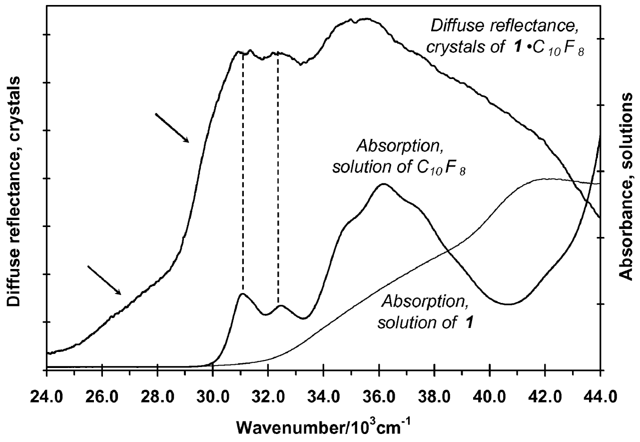

Fig. 5 Solid-state diffuse-reflectance spectrum of the **1**·$C_{10}F_8$ stacked adduct in comparison to its free molecular components, represented by dilute solutions of **1** and octafluoronaphthalene in acetonitrile.

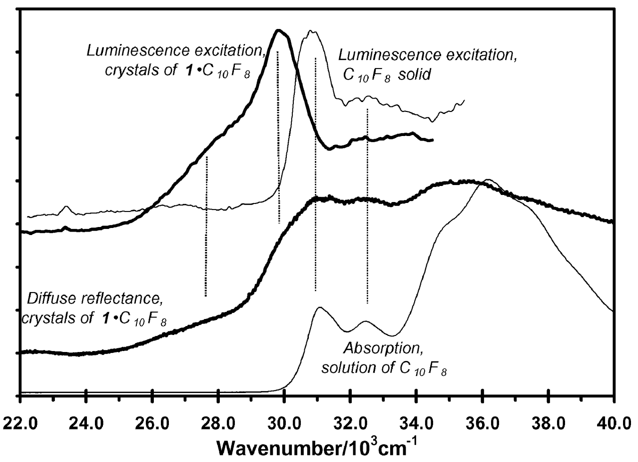

Fig. 6 Overlay of various electronic spectra of **1**·$C_{10}F_8$ and free $C_{10}F_8$ for purposes of comparison.

alone, which exhibits luminescence excitation peaks at shorter wavelengths and correspond to the monomer absorption peaks in the absorption spectrum of dilute solutions of $C_{10}F_8$.

We assign the diffuse-reflectance/excitation peaks at ~335 and 360 nm for **1**·$C_{10}F_8$ to charge-transfer transitions in the ground-state adduct. The trinuclear Au(I) complex **1** is strongly nucleophilic,[19] so it acts as a π-base and donates electron density to the π-acid $C_{10}F_8$. The resulting charge-transfer adduct exhibits characteristic absorptions that are red-shifted from the absorptions of its individual components. Kisch *et al.* suggested that donor-to-acceptor charge transfer bands should appear in the diffuse-reflectance spectra of 1 : 1 donor–acceptor inorganic–organic solid stacks.[44] Also, previous work by us[20] and by Balch and co-workers[12*b*] showed that charge-transfer absorption bands in the visible and near-IR region arise in *neutral* adducts that form upon interaction of trinuclear Au(I) complexes with organic acceptors such as TCNQ and nitro-substituted fluorenones. No luminescence data were reported in these previous reports, but they support the charge-transfer assignment of the lowest-energy diffuse-reflectance/excitation peaks of **1**·$C_{10}F_8$. Although the mechanism of the external heavy-atom effect of organic luminophores has been subject to numerous interpretations[45] and there seems to be lack of consensus on its origin, it has been suggested that charge transfer might play a role in the external heavy-atom effect. Evidence to this effect has been gathered, typically by analysis of the emission data for rigid glasses at cryogenic temperatures for a number of related luminophores that contain one or more heavy atoms (usually halogens), or by theoretical studies.[45] But, to our knowledge, distinct peaks due to the suggested charge-transfer process in the ground-state adduct, like those shown in Figs. 5 and 6, have not been reported for conventional organic luminophores that exhibit phosphorescence due to an external heavy-atom effect.

The conventional heavy-atom effect in organic molecules usually invokes a phosphorescence route that entails simply the enhancement of the S_1–T_1 intersystem crossing of the organic compound following direct absorption from S_0 to either S_1 or a higher singlet (*e.g.* S_2) that then relaxes to S_1 *via* internal conversion.[34,35] In contrast, the spectral data for the **1**·$C_{10}F_8$ adduct here suggest a different excitation route for the phosphorescence, as depicted in Fig. 7. Absorption occurs directly to the resulting charge-transfer states in the **1**·$C_{10}F_8$ adduct. The significantly lower intensity of the lowest-energy feature near 360 nm in the diffuse reflectance and excitation spectra of the adduct is consistent with a triplet charge transfer state (^{3}CT) while the stronger higher-energy feature near 335 nm is assigned to a singlet charge transfer state (^{1}CT). Fortunately, these charge transfer states lie higher in energy than the energy of the T_1 state of the organic component such that the latter state will not be depopulated as a result of the charge transfer process. Thus, the lowest-energy emitting state in the adduct remains as the T_1 state with little perturbation of its original energy in the organic component alone. The spectral data suggest that the S_1 state of $C_{10}F_8$ is not involved in the charge transfer process because vibronic features corresponding to this state remain essentially unperturbed in the electronic spectrum of the binary adduct (see the dashed lines in Fig. 5). Hence, we illustrate in Fig. 7 that the ^{3}CT and ^{1}CT states arise from the molecular orbital interaction of the T_2 and S_2 states of $C_{10}F_8$ with suitable frontier orbitals in **1** while both the S_1 and T_1 states of $C_{10}F_8$ remain non-bonding in the **1**·$C_{10}F_8$ adduct. The luminescence excitation spectrum that monitors the yellow phosphorescence of **1**·$C_{10}F_8$ (Fig. 6) suggests that the charge transfer process represents the major low-energy excitation route while excitation peaks due to direct absorption to the triplet are absent (*e.g.*, $S_0 \rightarrow T_1$ absorptions for naphthalenes lie in the range (20–25) × 10^3 cm^{-1}).[35] Finally, we would like to address the different luminescence behavior seen here for the **1**·$C_{10}F_8$ adduct from that of the **1**·C_6F_6 adduct we reported earlier,[20] which does not exhibit phosphorescence from the T_1 state of C_6F_6 on complexation with **1**. An explanation may lie in the fact that previous experimental data in the organic literature suggest that hexafluorobenzene has a greater ground to excited state separation than octafluoronaphthalene, leading to an increased internal conversion rate, $S_1 \rightarrow S_0$, for hexafluorobenzene compared to intersystem crossing, $S_1 \rightarrow T_1$, which dominates in octafluoronaphthalene; for further details, see refs. 30 and 46.

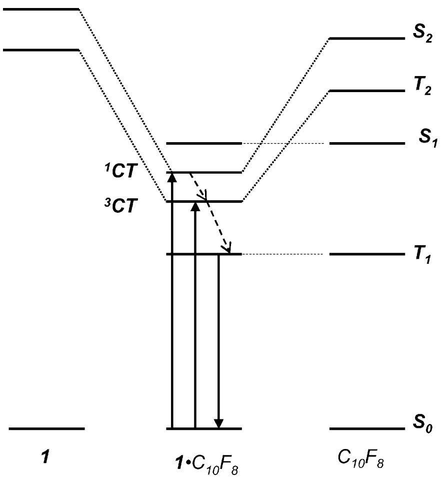

Fig. 7 Proposed energy level diagram showing the interaction between the excited states of **1** and $C_{10}F_8$ to form the charge transfer (CT) states in the **1**·$C_{10}F_8$ adduct.

Concluding remarks

This work demonstrates the extension of the range of applications resulting from the electron-rich nature of cyclic trinuclear Au(I) complexes to include the synthesis of bright room-temperature phosphors upon selective interaction with luminescent aromatic molecules that are electron poor. In addition to the fundamental significance in acid–base chemistry, the results of this work demonstrate a potential application in molecular light-emitting diodes because of the desired features for adducts like **1**·$C_{10}F_8$ as emitting materials for such devices,[47] including: (1) bright emission in the solid state at room temperature, (2) phosphorescent instead of fluorescent emission; the theoretical upper limit for the internal electroluminescence efficiency is 0.25 and 1.00 for fluorescent and phosphorescent materials, respectively, (3) the luminescence is sensitized by the intermolecular interactions in the solid state, where such interactions normally cause self-quenching in common luminophores, and (4) the 1 : 1 acid–base stacking pattern renders desirable charge transport properties of electrons and holes. Nevertheless, the relatively long lifetimes and the crystalline as opposed to amorphous nature of the solid are considered disadvantages for adducts like **1**·$C_{10}F_8$ with respect to certain display applications.

Acknowledgements

The financial support of this project has been provided by the Robert A. Welch Foundation of Houston, TX, to J. P. F. and M. A. O., a National Science Foundation CAREER award to M. A. O. (CHE-0349313), and an Advanced Technology Program grant from the Texas Higher Education Coordinating Board to M. A. O. We also thank Professor Alfredo Burini of the University of Camerino for initiating collaborative studies with the trinuclear Au(I) complexes.

References

1 J. K. Bera and K. R. Dunbar, *Angew. Chem., Int. Ed.*, 2002, **41**, 4453.

2 R. Hoffmann, *Angew. Chem., Int. Ed. Engl.*, 1987, **26**, 846.

3 *Extended Linear Chain Compounds*, ed. J. S. Miller, Plenum Press, New York, 1982, vol. 1–3.

4 Y. Kunugi, K. R. Mann, L. L. Miller and C. L. Exstrom, *J. Am. Chem. Soc.*, 1998, **120**, 589.

5 M. A. Mansour, W. B. Connick, R. J. Lachicotte, H. J. Gysling and R. Eisenberg, *J. Am. Chem. Soc.*, 1998, **120**, 1329.

6 (*a*) E. J. Fernandez, J. M. Lopez-de-Luzuriaga, M. Monge, M. E. Olmos, J. Perez, A. Laguna, A. A. Mohamed and J. P. Fackler, Jr., *J. Am. Chem. Soc.*, 2003, **125**, 2022; (*b*) E. J. Fernández, J. M. López-de-Luzuriaga, M. Monge, M. Montiel, M. E. Olmos, J. Pérez, A. Laguna, F. Mendizabal, A. A. Mohamed and J. P. Fackler, Jr., *Inorg. Chem.*, 2004, **43**, 3573–3581.

7 W. R. Caseri, H. D. Chanzy, K. Feldman, M. Fontana, P. Smith, T. A. Tervoort, J. G. Goossens, E. W. Meijer, A. P. Schenning, I. P. Dolbyna, M. G. Debije, M. P. de Haas, J. M. Warman, A. M. van de Craats, R. H. Friend, H. Sirringhaus and N. Stutzmann, *Adv. Mater.*, 2003, **15**, 125.

8 (*a*) H. Tanaka, Y. Okano, H. Kobayashi, W. Suzuki and A. Kobayashi, *Science*, 2001, **291**, 285; (*b*) F. Bigoli, P. Deplano, M. L. Mercuri, M. A. Pellinghelli, L. Pilia, G. Pintus, A. Serpe and E. F. Trogu, *Inorg. Chem.*, 2002, **41**, 5241; (*c*) N. Robertson and L. Cronin, *Coord. Chem. Rev.*, 2002, **227**, 93.

9 B. W. Smucker, J. M. Hudson, M. A. Omary and K. R. Dunbar, *Inorg. Chem.*, 2003, **42**, 4714.

10 M. A. Rawashdeh-Omary, M. A. Omary and J. P. Fackler, Jr., *Inorg. Chim. Acta*, 2002, **334**, 376.

11 M. Stender, R. L. White-Morris, M. M. Olmstead and A. L. Balch, *Inorg. Chem.*, 2003, **42**, 4504.

12 (*a*) J. C. Vickery, M. M. Olmstead, E. Y. Fung and A. L. Balch, *Angew. Chem., Int. Ed. Engl.*, 1997, **36**, 1179; (*b*) M. M. Olmstead, F. Jiang, S. Attar and A. L. Balch, *J. Am. Chem. Soc.*, 2001, **123**, 3260; (*c*) A. Hayashi, M. M. Olmstead, S. Attar and A. L. Balch, *J. Am. Chem. Soc.*, 2002, **124**, 5791.

13 M. R. Haneline, M. Tsunoda and F. P. Gabbaï, *J. Am. Chem. Soc.*, 2002, **124**, 3737.

14 M. A. Omary, R. M. Kassab, M. R. Haneline, O. Elbjeirami and F. P. Gabbaï, *Inorg. Chem.*, 2003, **42**, 2176.

15 (*a*) H. V. Dias, H. V. Diyabalanage, M. A. Rawashdeh-Omary, M. A. Franzman and M. A. Omary, *J. Am. Chem. Soc.*, 2003, **125**, 12072; (*b*) H. V. R. Dias, H. V. K. Diyabalanage, M. G. Eldabaja, O. Elbjeirami, M. A. Rawashdeh-Omary and M. A. Omary, *J. Am. Chem. Soc.*, 2005, **127**, 7489.

16 A. Burini, R. Bravi, J. P. Fackler, Jr., R. Galassi, T. A. Grant, M. A. Omary, B. R. Peitroni and R. J. Staples, *Inorg. Chem.*, 2000, **39**, 3158.

17 A. Burini, J. P. Fackler, Jr., R. Galassi, B. R. Pietroni and R. J. Staples, *Chem. Commun.*, 1998, 95.

18 A. Burini, J. P. Fackler, Jr., R. Galassi, A. Macchioni, M. A. Omary, M. A.-O. Rawashdeh, B. R. Pietroni, S. Sabatini and C. Zuccaccia, *J. Am. Chem. Soc.*, 2002, **124**, 4570.

19 A. Burini, J. P. Fackler, Jr., R. Galassi, T. A. Grant, M. A. Omary, M. A. Rawashdeh-Omary, B. R. Pietroni and R. J. Staples, *J. Am. Chem. Soc.*, 2000, **122**, 11264.

20 M. A. Rawashdeh-Omary, M. A. Omary, J. P. Fackler, Jr., R. Galassi, B. R. Pietroni and A. Burini, *J. Am. Chem. Soc.*, 2001, **123**, 9689.

21 For reviews, see: (*a*) A. Burini, A. A. Mohamed and J. P. Fackler, Jr., *Comments Inorg. Chem.*, 2003, **24**, 253; (*b*) M. A. Omary, A. A. Mohamed, M. A. Rawashdeh-Omary and J. P. Fackler, Jr., *Coord. Chem. Rev.*, 2005, DOI: 10.1016/j.ccr.2004.12.018.

22 F. Bonati, A. Burini, B. R. Pietroni and B. Bovio, *J. Organomet. Chem.*, 1989, **375**, 147.

23 *SMART V 4.043. Software for the CCD Detector System*, Bruker Analytical X-ray Systems, Madison, WI, 1995.

24 *SAINT V 4.035. Software for the CCD Detector System*, Bruker Analytical X-ray Systems, Madison, WI, 1995.

25 SADABS. Program for absorption corrections using Siemens CCD based on the method of Robert Blessing: R. H. Blessing, *Acta Crystallogr., Sect. A*, 1995, **51**, 33.

26 G. M. Scheldrick, *SHELXS-97. Program for the Solution of Crystal Structures*, University of Göttingen, Germany, 1997.

27 *SHELXTL 5.03 (PC-Version), Program Library for Structure Solution and Molecular Graphics*, Bruker Analytical X-ray Systems, Madison, WI, 1995.

28 Y. Xie, H. F. Schaefer and F. A. Cotton, *Chem. Commun.*, 2003, 102.

29 J. C. Miller, J. S. Meek and S. J. Strickler, *J. Am. Chem. Soc.*, 1977, **99**, 8175, and references therein.

30 H. B. Rosenberg and S. D. Carson, *J. Phys. Chem.*, 1968, **72**, 3531.

31 V. L. Ermolaev and K. J. Svitashev, *Opt. Spektrosk.*, 1959, **7**, 664.

32 E. F. Kiefer, W. L. Waters and D. A. Carlson, *J. Am. Chem. Soc.*, 1968, **90**, 5127.

33 W. Kitching, G. M. Drew and V. Alberts, *Organometallics*, 1982, **1**, 331.

34 (*a*) N. J. Turro, *Modern Molecular Photochemistry*, Benjamin/Cummings, Menlo Park, CA, 1978; (*b*) G. Kavarnos, T. Cole, P. Scribe, J. C. Dalton and N. J. Turro, *J. Am. Chem. Soc.*, 1971, **93**, 1032.

35 S. P. McGlynn, T. Azumi and M. Kinoshita, *Molecular Spectroscopy of the Triplet State*; Prentice-Hall, Englewood Cliffs, NJ, 1969.

36 D. S. McClure, N. W. Blake and P. L. Hanst, *J. Chem. Phys.*, 1954, **22**, 255.

37 V. L. Ermolaev and K. J. Svitashev, *Opt. Spektrosk.*, 1959, **7**, 399.

38 M. Kasha, *J. Chem. Phys.*, 1952, **20**, 71.

39 J. S. Griffith, *Theory of Transition Metal Ions*, Cambridge University Press, Cambridge, 1964.

40 J. Friedrich, F. Metz and F. Dörr, *Mol. Phys.*, 1975, **30**, 289.

41 H.-Y. Chao, W. Lu, Y. Li, M. C. Chan, C.-M. Che, K.-K. Cheung and N. Zhu, *J. Am. Chem. Soc.*, 2002, **124**, 14696.

42 M. A. Omary, M. A. Rawashdeh-Omary, H. V. Diyabalanage and H. V. Dias, *Inorg. Chem.*, 2003, **42**, 8612.

43 For reviews, see: (*a*) J. M. Forward, J. P. Fackler, Jr. and Z. Assefa, Photophysical and Photochemical Properties of Gold(I) Complexes, in *Optoelectronic Properties of Inorganic Compounds*, ed. D. M. Roundhill and J. P. Fackler, Jr., Plenum, New York, 1999, ch. 6; (*b*) V. W. Yam and K. K. Lo, *Chem. Soc. Rev.*, 1999, **28**, 323.

44 (*a*) H. Kisch, B. Eisen, R. Dinnebier, K. Shankland, W. I. David and F. Knoch, *Chem. Eur. J.*, 2001, **7**, 738; (*b*) H. Kisch, *Comments Inorg. Chem.*, 1994, **16**, 113.

45 There are too many reports to give a comprehensive citation about the mechanism of the external heavy-atom effect. For representative examples, see the following, and references therein: (*a*) T. Azumi, *Chem. Phys. Lett.*, 1973, **19**, 580; (*b*) A. K. Chandra, N. J. Turro, A. L. Lyons and P. Stone, *J. Am. Chem. Soc.*, 1978, **100**, 4964; (*c*) B. F. Minaev, S. Knuts and H. Ågren, *Chem. Phys. Lett.*, 1994, **181**, 15; (*d*) N. Chattopadhyay, C. Serpa, M. M. Pereira, J. Seixas de Melo, L. G. Arnaut and S. J. Formosinho, *J. Phys. Chem. A*, 2001, **105**, 10025; (*e*) I. R. Gould, J. A. Boiani, E. B. Gaillard, J. L. Goodman and S. Farid, *J. Phys. Chem. A*, 2003, **107**, 3515.

46 D. Phillips, *J. Chem. Phys.*, 1967, **46**, 4679.

47 For a review, see: S. Sibley, M. E. Thompson, P. E. Burrows and S. R. Forrest, Electroluminescence in Molecular Materials, in *Optoelectronic Properties of Inorganic Compounds*, ed. D. M. Roundhill and J. P. Fackler, Jr., Plenum, New York, 1999, ch. 2.